Synthesis and Photoinduced Electron-Transfer Properties of Phthalocyanine–[60]Fullerene Conjugates

Maurizio Quintiliani,[a] Axel Kahnt,[b] Thorsten Wölfle,[c] Wolfgang Hieringer,*[c] Purificación Vázquez,[a] Andreas Görling,[c] Dirk M. Guldi,*[b] and Tomás Torres*[a]

Dedicated to Professor Ulrich Nickel on the occasion of his retirement

Abstract: A series of three novel ZnPc–C_{60} conjugates (Pc = phthalocyanine) **1a–c** bearing different spacers (single, double, and triple bond) between the two electroactive moieties was synthesized and compared to that of ZnPc–C_{60} conjugate **2**, in which the two electroactive moieties are linked directly. The synthetic strategy—towards the preparation of **1a–c**—involved palladium-catalyzed cross-coupling reactions over a monoiodophthalocyanine precursor **4** to introduce the corresponding spacer, and subsequent dipolar cycloaddition reaction to C_{60}. Detailed photophysical investigations of **1a–c** and **2** prompted an intramolecular electron transfer that evolves from the photoexcited ZnPc to the electron-accepting C_{60}. In particular, with the help of femtosecond laser photolysis charge separation was indeed confirmed as the major deactivation channel. Complementary time-dependent density functional calculations supported the spectral assignment, namely, the spectral identity of the ZnPc$^{•+}$ radical cation and the $C_{60}{}^{•-}$ radical anion as seen in the differential absorption spectra. The lifetimes of the correspondingly formed radical ion-pair states depend markedly on the solvent polarity: they increase as polarity decreases. Similarly, although to a lesser extent, the nature of the linker impacts the lifetime of the radical ion-pair states. In general, the lifetimes of these states tend to be shortest in the system that lacks any spacer at all (**2**), whereas the longest lifetimes were found in the system that carries the triple-bond spacer (**1a**).

Keywords: charge transfer · conjugation · density functional calculations · fullerenes · phthalocyanines

[a] Dr. M. Quintiliani, Prof. P. Vázquez, Prof. T. Torres
Departmento de Química Orgánica
Universidad Autónoma de Madrid
Cantoblanco, 28049, Madrid (Spain)
Fax: (+34) 914-973-966
E-mail: tomas.torres@uam.es

[b] A. Kahnt, Prof. D. M. Guldi
Department of Chemistry and Pharmacy &
Interdisciplinary Center for Molecular Materials
Friedrich-Alexander-Universität Erlangen-Nürnberg
91058 Erlangen (Germany)
Fax: (+49) 9131-852-8307
E-mail: dirk.guldi@chemie.uni-erlangen.de

[c] T. Wölfle, Dr. W. Hieringer, Prof. A. Görling
Department of Chemistry and Pharmacy &
Interdisciplinary Center for Molecular Materials
Institute for Physical and Theoretical Chemistry
Friedrich-Alexander-Universität Erlangen-Nürnberg
91058 Erlangen (Germany)
Fax: (+49) 9131-852-7736
E-mail: hieringer@chemie.uni-erlangen.de

Supporting information for this article is available on the WWW under http://www.chemeurj.org/ or from the author.

Introduction

In photosynthesis, cascades of short-range energy-transfer and electron-transfer events occur between well-arranged organic pigments (light-harvesting antenna ensemble and photosynthetic reaction center (PRC)) and other cofactors.[1a] Thereby the antenna portion captures light and transduces the resulting excitation energy, by means of singlet–singlet energy transfer, to the PRC. In the PRC charges are then separated with remarkable efficiency to yield a spatially and electronically well-isolated radical pair. Key to this success is, without any doubt, the overall small reorganization energy ($\lambda \approx 0.2$ eV) exhibited by the PRC and the well-balanced electronic coupling between each donor and acceptor. The arrangement of the donor–acceptor couples in the PRC is simple and accomplished through their noncovalent incorporation into well-defined transmembrane proteins. Owing to the importance and complexity of natural photosynthesis, the study thereof necessitates suitable simpler models. The ultimate goal is to design and assemble ar-

tificial systems that can efficiently process solar energy, replicating the natural analogue.[1b] In the last decades the development of artificial photosynthetic systems mimicking the natural process for solar-energy conversion and exploitation of molecular devices has attracted great interest.[1] An important approach to achieve this goal is the development of electron-donor and -acceptor chromophores linked by well-defined spacers.[2] The role played by the different spacer is not just structural, as its chemical nature governs the electronic communication between the terminal units. Another important feature of the spacer is its modular composition, which allows one to alter the separation without affecting the electronic nature of the connection.

Fullerenes have a three-dimensional, spherical structure consisting of alternating hexagons (electron rich) and pentagons (electron deficient) with diameters starting at 7.8 Å for C_{60}. Thus, it is interesting to relate their properties to conventional two-dimensional π-systems. Their extraordinary electron-acceptor properties—predicted theoretically and confirmed experimentally—have resulted in significant advances in the areas of light-induced electron-transfer chemistry and solar-energy conversion. It is mainly the small reorganization energy that fullerenes exhibit in electron-transfer reactions that is accountable for a noteworthy breakthrough. In particular, ultrafast charge separation together with very slow charge-recombination features lead to unprecedented long-lived radical ion-pair states formed in high quantum yields.[3] As the electron-donor partner, porphyrins are among the most frequently studied components.[4] On the other hand, synthetic porphyrin analogues such as phthalocyanines (Pcs)[5] present the advantage of exhibiting very high extinction coefficients within a wavelength range that extends to around 700 nm. Consequently, Pcs have emerged as excellent light-harvesting antennas for the incorporation into donor–acceptor systems, especially for harvesting the red part of the solar spectrum. Torres, Guldi, and others have developed a wide facet of donor–acceptor multicomponent systems that are based on phthalocyanines.[6] Although several examples of covalent[7] and supramolecular[8] phthalocyanine–fullerene systems for light harvesting have been reported by us, photoinduced electron transfer in Pc–C_{60} ensembles is not yet fully understood. The current work is expected to make a significant contribution to this field of research.

In this context, we present herein the synthesis and photophysical properties of a set of three ZnPc–C_{60} conjugates **1a–c** bearing different spacers (single, double, and triple bond, see Figure 1). To evaluate the impact of the spacer in the electron-transfer process, we have included the photophysical and theoretical characterization of directly linked ZnPc–C_{60} conjugate **2**[7b,e] under the same measurement conditions, employing vinyl-Pc **3**[7b] as a reference compound.
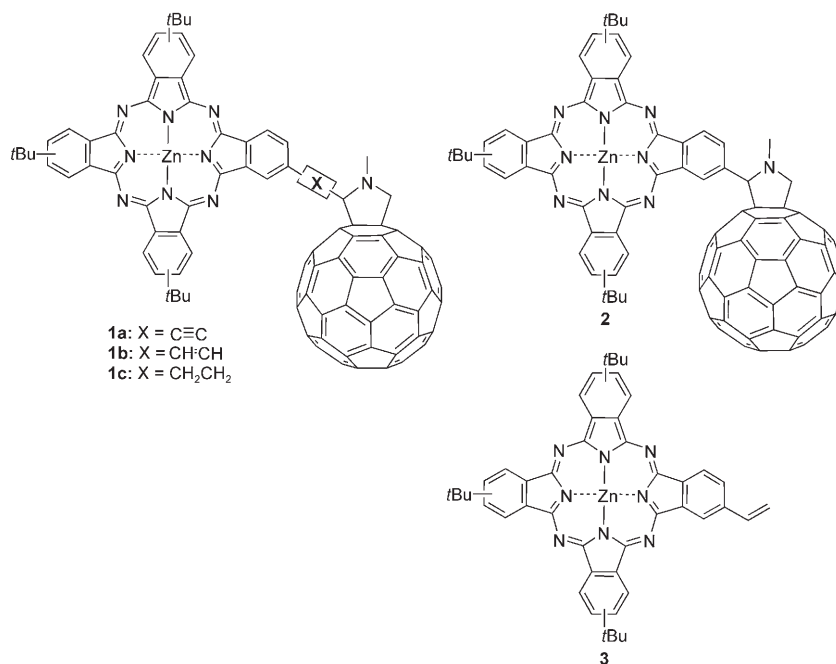

Figure 1. Structure of ZnPc–C_{60} conjugates (**1a–c** and **2**) and ZnPc reference compound **3**.

Results and Discussion

Synthesis and characterization: The synthetic strategy towards ZnPc–C_{60} conjugates **1a–c** consisted of the preparation of the precursor formyl-phthalocyanines **6–8**, followed by Prato reaction with C_{60} and sarcosine (Scheme 1).

The synthesis of formyl-Pc **6** was carried out starting from iodophthalocyanine precursor **4**,[9] which was subjected to a Sonogashira cross-coupling reaction with propargyl alcohol in the presence of Et₃N, THF, and a catalytic amount of [Pd-(PPh₃)₂Cl₂] and CuI, yielding 63% of derivative **5**. Subsequent oxidation of **5** with pyridinium chlorochromate (PCC) led to **6** in 47% yield. The search for a suitable synthetic strategy towards the preparation of **7** required the examination of several methods. Direct reduction of the triple bond of **6** was excluded, because it would involve reaction conditions that would challenge the integrity of the Pc. Moreover, even if this procedure provided **7**, it would be difficult to separate this from the precursor **6**, because both of these compounds present the same front (R_f) in thin layer chromatography (TLC) (see below). In this regard, we decided to employ a Pd-mediated methodology.
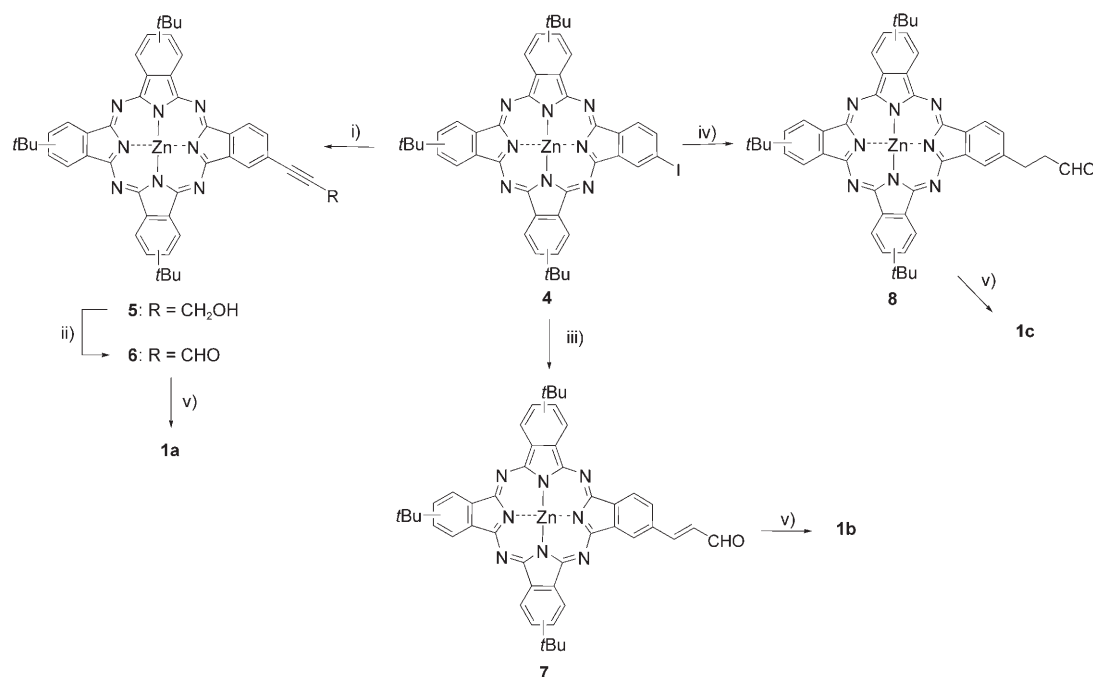
Scheme 1. Synthesis of ZnPc–C$_{60}$ conjugates **1a–c**. i) HC≡CCH$_2$OH, [Pd(PPh$_3$)$_2$Cl$_2$], CuI, THF, Et$_3$N, RT (63%); ii) PCC, CH$_2$Cl$_2$, RT (47%); iii) acrolein, [Pd(OAc)$_2$], NaHCO$_3$, Bu$_4$NCl, DMF, 20°C (91%); iv) allylic alcohol, [Pd(OAc)$_2$], NaHCO$_3$, Bu$_4$NCl, DMF, 30°C (76%); v) C$_{60}$, sarcosine, toluene, reflux.

Our initial plan was to perform a Heck reaction between **4** and an acrolein acetal, namely, 2-vinyl-1,3-dioxolane. However, this procedure is flawed by the formation of mixtures of the desired vinylic substitution products and ester derivatives from the carbopalladation intermediate, as reported in literature.[10] Therefore, Heck reaction of **4** with acrolein was envisaged as a useful and straightforward approach to compound **7**. Following the Jeffery protocol,[11] Pc **7** was synthesized by palladium-catalyzed vinylic substitution of acrolein with **4**, in the presence of NaHCO$_3$, nBu$_4$NCl, DMF, and a catalytic amount of [Pd(OAc)$_2$] at 20°C in 91% yield. The synthesis of formyl-Pc **8** involved Heck arylation of allylic alcohol with **4** according to the above-mentioned Jeffery conditions,[12] in 76% yield. Formyl-phthalocyanines **6–8** were finally subjected to a 1,3-dipolar cycloaddition with C$_{60}$ and sarcosine in refluxing toluene to afford conjugates **1a–c** in 20, 23, and 21% yields, respectively, after purification by column chromatography on silica gel using toluene/ethyl acetate mixtures as eluent.

All new compounds were characterized by MALDI-TOF mass spectrometry, ^{1}H NMR, UV-visible, and FTIR spectroscopies. Molecular ions were observed by mass spectrometry, whereas peaks corresponding to [M−C$_{60}$]$^+$ fragments were present in the spectra of **1a–c**. The ^{1}H NMR spectra showed the typical pattern of $tert$-butyl-Pcs with broad signals. In addition, the characteristic aldehyde signal appeared in the spectra of formyl-Pcs **6–8**, as well as signals corresponding to the pyrrolidine ring in the cases of **1a–c**.

Figure 2 summarizes the absorption spectra of formyl-Pcs **5–8** in CHCl$_3$. Interestingly, whereas in Pcs **5** and **8** a single Q-band is seen, Pcs **6** and **7** exhibit a splitting and red-shift
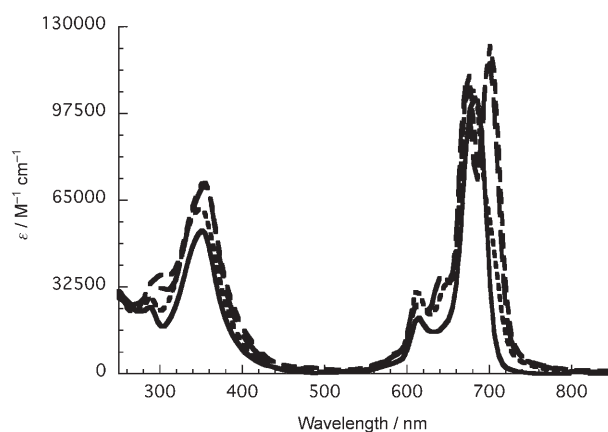

Figure 2. Absorption spectra of **5–8** in CHCl$_3$ (**5** ——, **6** – – –, **7** –·–·, **8** ·····).

of the Q-band in two equally intense peaks resulting from the extended π-conjugation. The UV-visible spectra of ZnPc–C$_{60}$ conjugates **1a–c** in CHCl$_3$ are compared in Figure 3. With respect to the positions of the Q-band, **1a** and **1b** exhibit shifts to higher wavelengths relative to **1c**. This is in agreement with extending the π-conjugation, especially for the conjugate with the ethynyl spacer. On the other hand, the weak absorption observed at 330 nm is characteristic of the [6,6] monoadduct of C$_{60}$.

ZnPc reference: The optical absorption features of ZnPc **3** were recorded in a variety of solvents (toluene, anisole, THF, and benzonitrile). At first glance, **3** exhibits in all sol-
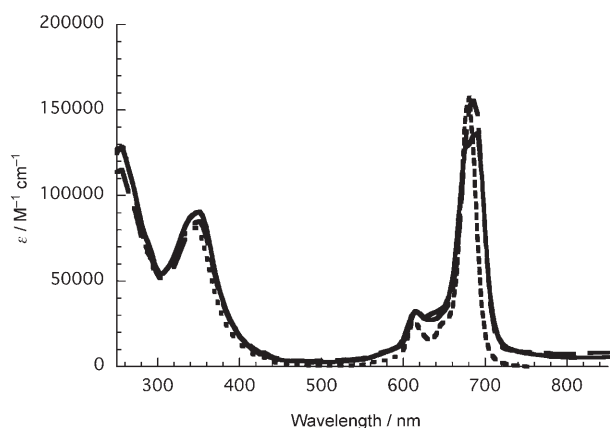
Figure 3. Absorption spectra of **1a–c** in CHCl₃ (**1a** ——, **1b** –––, **1c** ·····).

vents a set of Q-bands, that is, a strong maximum at around 685 nm flanked by a minor maximum at around 610 nm, and a Soret-band that maximizes at 350 nm. The spectroscopic features of the ZnPc Q- and Soret-bands relate to S_0–S_1 and S_0–S_2 transitions, respectively.[13]

Compound **3** emits strongly in the monitored range between 620 and 800 nm (Figure S1). This emission, which originates from the ZnPc singlet excited state, is strong (a quantum yield of 0.3)[14] and relatively long-lived (a lifetime of 3.1 ns). With the help of the long-wavelength absorption and the short-wavelength fluorescence we have determined the singlet excited-state energy as 1.8 eV.[8g,h] The corresponding ZnPc triplet excited state lies at around 1.2 eV. To shed light onto the spectral characteristics of the ZnPc singlet excited state, femtosecond-resolved transient absorption spectroscopy was employed. For **3**, differential absorption changes reveal in all solvents a maximum at 500 nm followed by a set of two minima that are located at 610 and 685 nm. These changes are attributed to the singlet–singlet absorptions of **3**. In **3**, the singlet–singlet features decay slowly to the corresponding triplet manifold. The main spectral feature of the latter is a rather broad transient species, for which a maximum at 490 nm (see below) was observed (Figure S2). To confirm the features of the long-lived triplet excited state, nanosecond-resolved transient absorption spectroscopy was employed. The differential absorption spectrum in THF is depicted as a representative example in Figure S3. It shows a set of two minima, one at around 350 nm and another at around 680 nm. These two minima are nice reflections of the Soret- and Q-band absorptions seen at 350 and 680 nm, respectively. In addition, the aforementioned 490 nm maximum is seen, which corresponds to a triplet–triplet transition. The underlying triplet character was corroborated by quenching with molecular oxygen. Although in the absence of molecular oxygen the triplet excited state of **3** decays with a rate constant of $3.5 \times 10^4 \, s^{-1}$ (THF), the presence of molecular oxygen leads to a nearly diffusion-controlled deactivation (Figure S4). All of these photophysical properties are in good agreement with those previously established by Bryce et al.[15]

ZnPc–C₆₀ conjugates: The electronic ground-state absorption spectra of the ZnPc–C₆₀ conjugates **1a–c** and **2** (Figure 3) resemble that of the ZnPc reference compound **3**: a strong maximum at around 685 nm is flanked by a minor maximum at around 610 nm (Q-bands), and a maximum at 350 nm (Soret-band). An additional band, with a 330 nm maximum, seen in the ZnPc–C₆₀ conjugates corresponds to a fullerene-centered transition.[16]

The spectroscopic absorption features of ZnPc and C₆₀ observed in the experiments were further analyzed by calculations using time-dependent density functional theory. Because the electronic structure and main excitations of ZnPc have been discussed in detail before,[13,17] we here focus only on the main features. The main features of the excitation spectrum are displayed in Figure 4 (black line, also
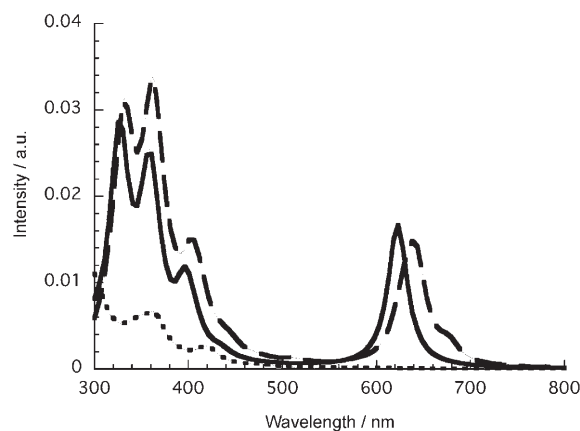

Figure 4. Calculated electronic absorption spectrum of ZnPc–C₆₀ (–––), ZnPc (——), and C₆₀ (·····).

Table S1) and all the important molecular orbitals of the ZnPc molecule are shown in Figure 5. In ZnPc, a strong band is calculated at 633 nm (experimental: 685 nm, 610 nm; Q-bands), which is assigned to a $2a_{1u}$ (HOMO) to $7e_g$ (LUMO) transition. Within the range of the 350 nm peak, several transitions were found in the calculations; the three most intensive peaks occurred at 329, 361, and 367 nm. These excitations contain large contributions from orbital transitions $1a_{1u} \rightarrow 7e_g$ (LUMO) and $2a_{1u}$ (HOMO) $\rightarrow$ $8e_g$ (Table S1). Notably, the intensity of the 625 and 350 nm bands are apparently reversed when compared to the experimental data (Figure 3). Overall, we find excellent agreement between the present calculations and those reported earlier by Ricciardi et al.[13]

The simulated absorption spectrum of C₆₀ is shown in Figure 4 (dotted line, see also Table S2). The most intensive part of the spectrum of C₆₀ is found in the UV range.[18] In contrast to pristine C₆₀ (data not shown), a set of moderately intensive excitations is found for the C₆₀ reference within the spectral range of 420 nm. The most intensive excitation corresponds to an orbital transition from the HOMO (196a), a π-type orbital that extends over both the pyrrolidine ring and the fullerene framework, to the LUMO+5
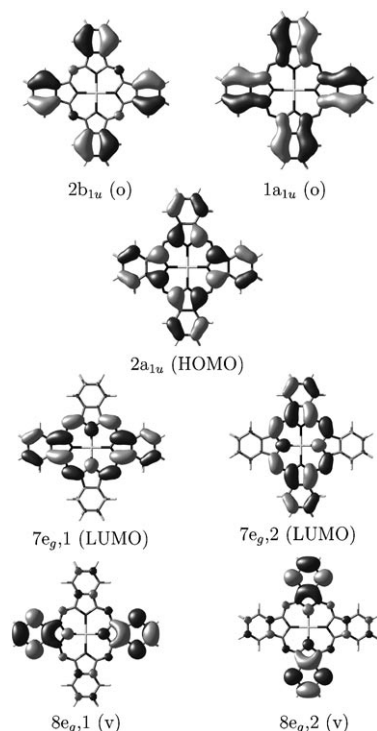
Figure 5. Selected molecular orbitals of ZnPc (D_{4h} symmetry); (o)/(v): occupied/virtual orbital.

(202a), localized predominantly at the methyl pyrrolidine ring (Figure 6). C_{60} exhibits, according to our calculations, no appreciable electronic transitions with an oscillator strength above 0.1 at energies below 450 nm. The low-energy part of the C_{60} spectrum will be discussed later in connection with that of the $C_{60}^{\bullet-}$ radical anion.
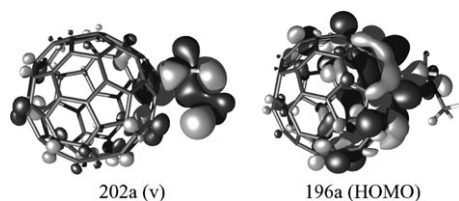

Figure 6. Selected molecular orbitals of C_{60}.

The computed absorption spectrum and corresponding details of salient electronic excitations of ZnPc–C_{60} **2** are shown in Figure 4 (dashed line, see also Table S3). Relevant molecular orbitals are shown in Figure 7. In general, the molecular orbitals of the conjugate show the expected resemblance to the ZnPc and C_{60} orbitals. Only a few orbitals extend over both the ZnPc and C_{60} moieties. The computed electronic excitation spectrum of ZnPc–C_{60} is, in line with the experiments, dominated by the ZnPc transitions. Peaks at 642 and 633 nm (labels 17A and 19A, "Q-bands", Table S3) are assigned to transitions from the HOMO (342a) to the nearly degenerate virtual orbitals 346a and 347a that are localized on ZnPc (i.e., descendant from the
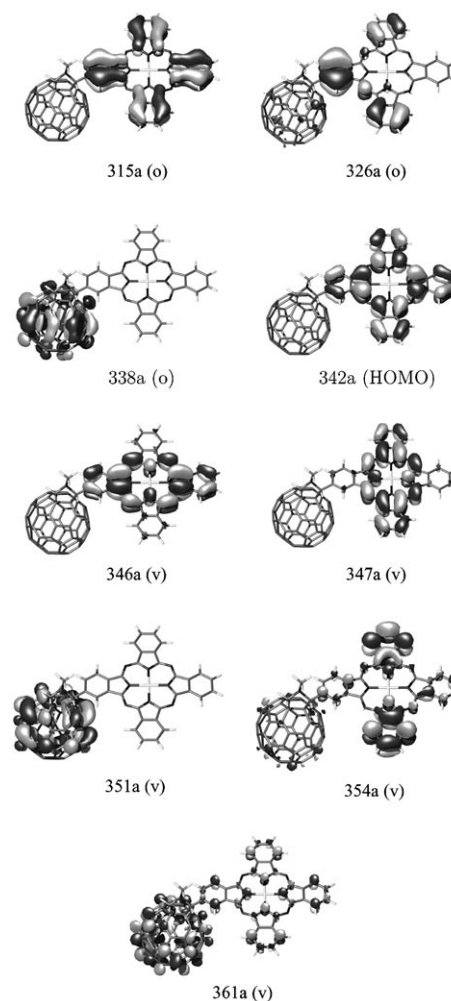

Figure 7. Selected molecular orbitals of ZnPc–C_{60} **2**; (o)/(v): occupied/virtual orbital.

$7e_g$ set in ZnPc). These excitations correspond to the degenerate $1E_u$ transitions in ZnPc (D_{4h} symmetry, "Q-band", $2a_{1u}$ (HOMO)→$7e_g$ orbital transition, Table S1), which, due to the loss of perfect D_{4h} symmetry in the conjugate, split into two close-lying excitations. Likewise, two further pairs of ZnPc excitations are assigned to transitions into the same set of virtual orbitals 346a/347a. The first pair labeled 118A/119A at 413/412 nm (Table S3 in the Supporting Information) reflects a dominant transition from occupied orbital 330a (not shown), which is reminiscent of the $6a_{2u}$ orbital in ZnPc (D_{4h}). The other pair of excitations at 405 and 402 nm (126A and 131A) is more intensive (Table S3). It is assigned to a transition from orbital 326a (Figure 7), which is asymmetric but may be considered as descendant from the $2b_{1u}$ orbital of ZnPc. Hence, the pair of excitations at 405 nm/ 402 nm likely corresponds to the $4E_u$ transition in ZnPc ("B_1-band", $2b_{1u}$→$7e_g$). The transition computed at an excitation wavelength of 366 nm (180A, "Soret"), which removes an electron from the HOMO of the ZnPc–C_{60}, corresponds to the $5E_u$ and/or $6E_u$ transitions at 363 and 357 nm in ZnPc.[19] At 332 and 355 nm, two excitations are computed that are largely centered on the fullerene moiety of the

conjugate (Table S3). At almost the same excitation wavelength of 330 nm, the calculations predict another intensive excitation that can be assigned to the "B_2 band" of ZnPc ($7E_u$). The expected properties of a charge-separated charge-transfer excited state of the **2** conjugate will be discussed below in terms of the radical fragments ZnPc$^{\cdot+}$ and $C_{60}^{\cdot-}$.

To test possible electron-donor–acceptor interactions that might dominate the excited-state deactivations in the ZnPc–C_{60} conjugates (**1a–c** and **2**) a series of steady-state and time-resolved assays were conducted. First evidence, although indirect, came from the quenching of the ZnPc-centered fluorescence. Besides minor changes in the fluorescence maximum (**3**: 690 nm; **1a**: 689 nm; **1b**: 681 nm; **1c**: 680 nm; **2**: 683 nm) the general shape of the fluorescence spectra is practically identical to that of the ZnPc reference (Figure 8). However, the intensities are more than one order of magnitude lower than seen in the ZnPc reference. In fact, in ZnPc–C_{60} **2**, which lacks a molecular spacer and in which ZnPc and C_{60} are directly connected, the fluorescence intensity was quenched by two orders of magnitude.
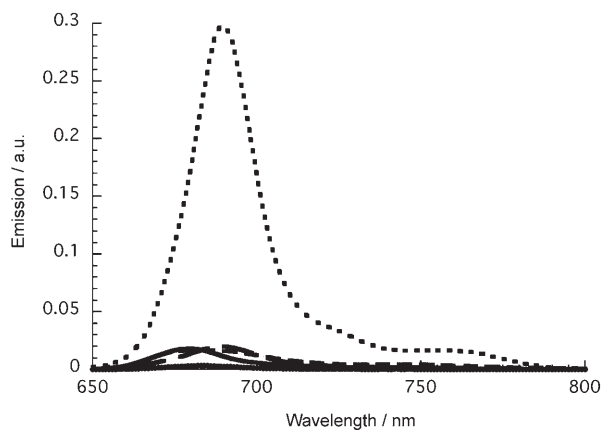

Figure 8. Fluorescence spectra of the reference (ZnPc **3**, ■) and the conjugates (**1a** – – –, **1b** –·–·, **1c** ·····, and **2** ——) in THF upon photoexcitation at 610 nm.

To shed light on the nature and dynamics of a possibly formed charge-separated radical ion-pair state, femtosecond-resolved transient absorption spectroscopy was employed. Hereby, ZnPc **3** and all ZnPc–C_{60} conjugates (**1a–c** and **2**) were probed under variable conditions.

Note that at very early times the transient absorption spectra, following photoexcitation of the ZnPc–C_{60} conjugates (**1a–c** and **2**), resemble those seen for the ZnPc reference **3**, which confirms the successful formation of the singlet excited ZnPc state in the conjugates. In stark contrast, the differential absorption changes decay rapidly to a new transient that reveals three distinct maxima at 520, 840, and 1000 nm. Whereas the bands at 520 and 840 nm are attributes of the one-electron-oxidized ZnPc radical cation,[20] the band at 1000 nm matches the absorption of the one-electron-reduced fullerene radical anion.[21] In summary, we pos-

tulate the formation of a radical ion-pair state that evolves from the photoexcited ZnPc. In Figure 9 and Figures S5–7 representative transient absorption spectra are gathered for **1a**, and for **2**, **1b**, and **1c**, respectively.
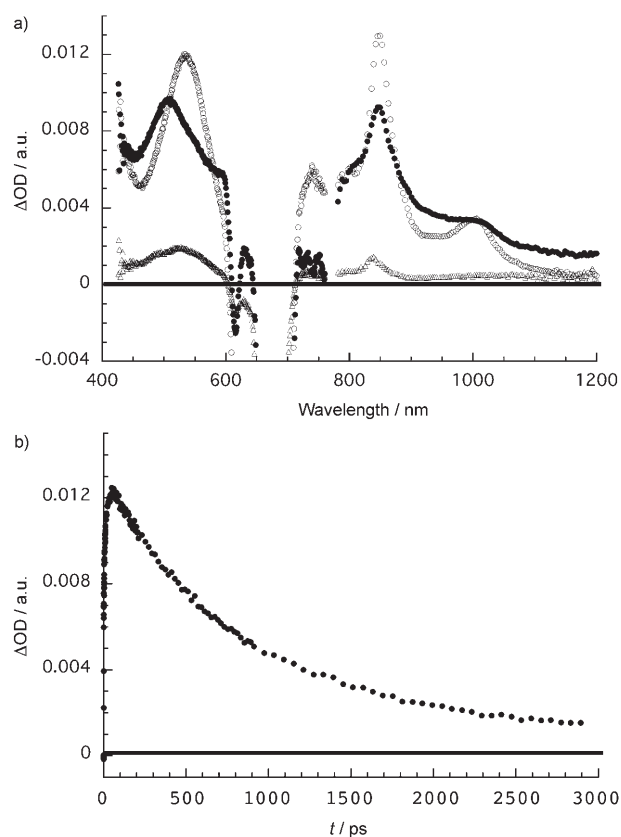

Figure 9. Top: differential absorption spectra (visible and near-infrared) obtained upon femtosecond flash photolysis (670 nm) of **1a** in nitrogen-saturated anisole with several time delays (1 ps ■; 102 ps □; 2892 ps △) at RT. Bottom: time-absorption profiles of the spectra shown above at 845 nm, monitoring the charge separation and charge recombination.

The quantum yields for charge separation were calculated taking the ZnPc **3** triplet ($\Phi = 0.7$, $\varepsilon = 28900 \, \text{M}^{-1} \, \text{cm}^{-1}$)[22] in THF and the methylene blue triplet ($\Phi = 0.5$, $\varepsilon = 14400 \, \text{M}^{-1} \, \text{cm}^{-1}$)[22,23] in methanol as references. The extinction coefficient of the one-electron-oxidized ZnPc$^{\cdot+}$ ($29000 \, \text{M}^{-1} \, \text{cm}^{-1}$) was taken from Ohno et al.[24] The calculated quantum yields for the formation of the charge-separated state are gathered in Table 1. Generally speaking, the quantum yields are high with the highest values in anisole and THF. In benzonitrile, on the other hand, they drop significantly with values as small as 0.56; a trend that is similar to previously studied donor–acceptor systems.[2] Relative to **2**, in which ZnPc and C_{60} are directly linked, the quantum yields drop upon implementation of the spacers in **1a**, **1b**, and **1c**, which is likely to relate to a weaker coupling.

Importantly, within the temporal limitations of our femtosecond experiments (3000 ps) both features of the radical ion-pair state, namely, the one-electron-reduced C_{60} radical anion and one-electron-oxidized ZnPc radical cation, exhibit

FULL PAPER

Table 1. Selected photophysical parameters of ZnPc–C_{60} conjugates.[a]

	Solvent	2	1a	1b	1c
lifetimes (τ) of radical ion-pair state [ps]	benzonitrile	32	36	30	50
	THF	49	154	120	131
	anisole	450	1204	979	755
	toluene	11 000	13 000	14 000	10 000
quantum yield (Φ) of radical ion-pair state formation	benzonitrile	0.68	0.56	0.58	0.64
	THF	≈ 1	0.65	0.68	0.78
	anisole	0.90	0.81	0.77	0.76

[a] Upper limit: the time resolution of the ns-laser photolysis system is 12 ns.

a strict mono-exponential decay. To probe the impact that the solvent polarity and the linker might impose on the radical ion-pair state lifetime, a variety of solvent polarities, ranging from toluene to benzonitrile, and the different spacers, namely, direct linkage (**2**), single (**1a**), double (**1b**), and triple bond (**1c**), were compared with each other. A few illustrative time-absorption profiles at 845 nm, which represent the decay of the one-electron-oxidized ZnPc radical cation, are shown in Figure 10 and Figures S8–10. The femtosecond laser photolysis transient absorption spectroscopy shows clearly that the lifetime of the radical ion-pair state depends strongly on the polarity of the solvent: the lifetime is longer in the less-polar solvents.
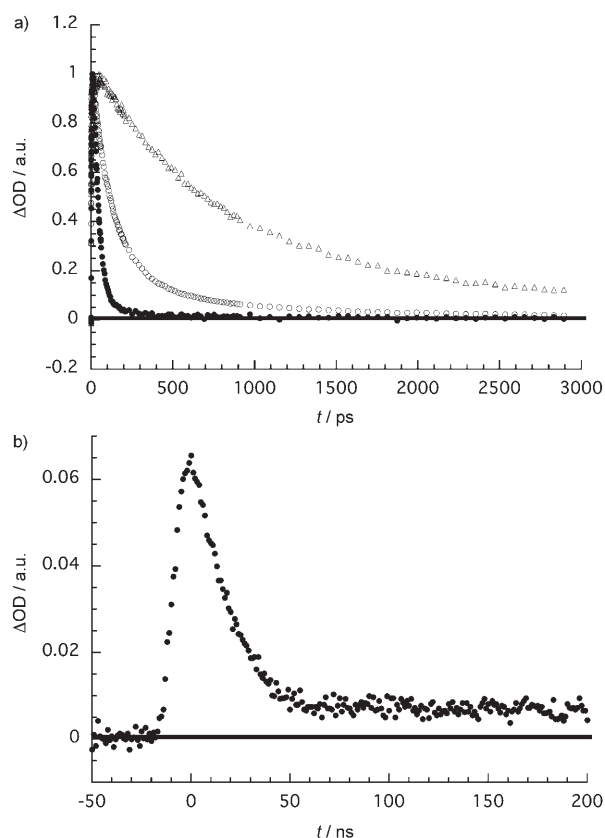

Figure 10. Top: time absorption profiles of the ZnPc radical cation band at 845 nm for **1a** in anisole ($\triangle$), in THF ($\square$), and in benzonitrile ($\blacksquare$). Bottom: time absorption profiles of the ZnPc radical cation band at 845 nm for **1a** in toluene.

In line with the Marcus theory of electron transfer,[25] the lifetime of the radical ion-pair state depends strongly on the polarity of the solvent. More precisely, as the solvent polarity decreases the charge-recombination dynamics are pushed deeper and deeper into the Marcus inverted region. Table 1 lists the lifetimes of the charge-separated states (**1a–c** and **2**).

From femtosecond and complementary nanosecond experiments we gather that the deactivation of the radical ion-pair state leads mainly through a non-radiative pathway to direct recovery of the singlet ground state. A minor deactivation channel ($\ll 5\%$) via the ZnPc triplet excited state cannot be excluded. Similarly, although to a lesser extent, the linker also impacts the lifetime. In general, the lifetime of the charge-separated state is shorter in the system that lacks a linker between the ZnPc and C_{60} moieties.

To scrutinize the differential absorption of the postulated radical ion pair, the electronic structure and the electronic absorption spectra of the ZnPc$^{\bullet+}$ radical cation and the $C_{60}^{\bullet-}$ radical anion were investigated theoretically. The low-energy part of the simulated electronic absorption spectrum of $C_{60}^{\bullet-}$ is shown in Figure 11 (dashed line). It is dominated by three major bands centered at 546, 809, and 989 nm (Table S4). Note that in the experimental spectra, three bands were detected at 520, 840, and 1000 nm. All three excitations contain dominant contributions from transitions between the singly occupied HOMO (labeled 197a, majority spin channel) and low-lying virtual π-orbitals. A comparison of the computed excitation spectra of the $C_{60}^{\bullet-}$ radical anion with that of neutral C_{60} at wavelengths above 400 nm (Figure 11) shows that all three major peaks discussed above are absent in the spectrum of the neutral C_{60} molecule. This is because these transitions start from the singly occupied HOMO (197a), which hosts the extra electron of the $C_{60}^{\bullet-}$ radical anion. On the other hand, the neutral C_{60} molecule features an excitation at 423 nm (see above, Table S2), which is absent in $C_{60}^{\bullet-}$.

The computed electronic absorption spectrum of ZnPc$^{\bullet+}$ shows two major features at 421 and 696 nm (Figure 12 dashed line, see also Table S5). The lower-energy excitations
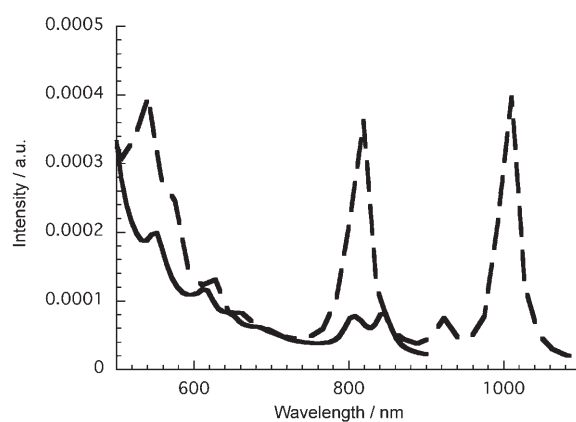

Figure 11. Low-energy part of the simulated electronic excitation spectrum of the $C_{60}^{\bullet-}$ radical anion (---) and neutral C_{60} (——).
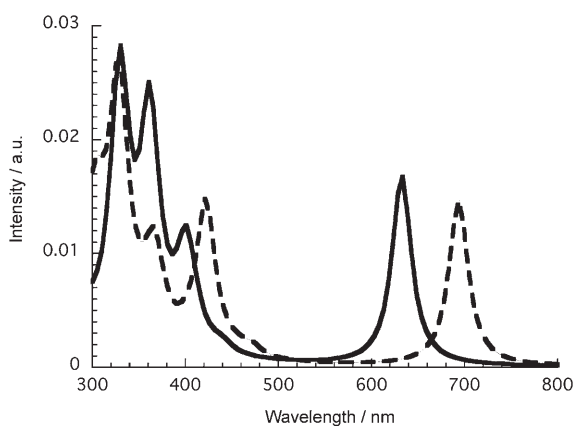
Figure 12. Simulated electronic absorption spectrum of ZnPc$^{\bullet+}$ (– – –) and ZnPc (——). Arbitrary units (a.u.) for intensity.

at 696 nm (10A and 11A in Table S5) originate from the singly occupied HOMO (147a, majority spin channel α), and thus correspond to the $2a_{1u} \rightarrow 7e_g$ transition of neutral ZnPc ($1E_u$, "Q-band", 623 nm, Table S1). The excitations at 421 nm (54A and 55A, see Table S5, minority spin channel β)[26] may be assigned to the $2b_{1u} \rightarrow 7e_g$ ($4E_u$, "B1 band", 397 nm) transition in neutral ZnPc. All of these excitations thus correspond to transitions into a set of four almost degenerate spin orbitals (148α/β, 149α/β) that are descendant from the $7e_g$ degenerate orbital set in neutral ZnPc (D_{4h} symmetry). A comparison of the computed absorption spectra of neutral ZnPc with that of the ZnPc$^{\bullet+}$ radical cation shows a strong red-shift for the lower-energy bands upon one-electron oxidation of ZnPc (see Figure 12). Note also that the excitations $5E_u$ and $6E_u$ of neutral ZnPc (Table S1) are computed at considerably higher energies (226 nm, data not shown), and, therefore, are not discussed here any further.

Nyokong et al. have reported excitation bands for ZnPc$^{\bullet+}$ in methylene chloride solution at 440, 500, 720 ("Q-band"), and 825 nm based on magnetic circular dichroism experiments.[20b] Admitting a shift of about 25 nm (due to solvent effects and/or inaccuracies in the calculations), the first and the third band mentioned above may be identified with our computed excitations at 421 nm ($4E_u$, "B1") and 696 nm ($1E_u$, "Q"). The weak shoulder at 472 nm in the simulated spectrum may correspond to the experimental band at 500 nm. Note that the present calculations do not predict any intensive excitation at wavelengths above 700 nm, that is, the oscillator strengths of these transitions are invariably below 0.001.

Conclusion

We have described the synthesis and photophysical properties of a set of three different ZnPc–C_{60} conjugates **1a–c** presenting different spacers. The synthetic strategy towards **1a–c** consisted of the preparation of the precursor formyl-phthalocyanines **6–8**, using palladium-mediated C–C cou-

pling methodologies, followed by cycloaddition reaction with C_{60} in the presence of sarcosine. The current study documents that an intramolecular charge transfer starting from the photoexcited ZnPc to the electron-accepting C_{60} governs the photoreactivity of **1a–c** and **2**. This yields, in turn, for all ZnPc–C_{60} conjugates the one-electron-oxidized ZnPc radical cation and the one-electron-reduced C_{60} radical anion. Initial charge-transfer evidence came from ZnPc fluorescence quenching experiments upon comparison of, for example, **1a–c** and **2** with a ZnPc reference **3**. Because the fluorescence quantum yield of ZnPc is well established with a value of 0.3,[14] we used ZnPc as a reference to determine the fluorescence quantum yields in the ZnPc–C_{60} conjugates. The calculated fluorescence quantum yields, following 610 nm photoexcitation, are for THF: **1a** = 0.023; **1b** = 0.03; **1c** = 0.02; **2** = 0.003. Additional charge-transfer evidence is based on spectroscopic studies. In particular, femtosecond laser photolysis has clearly helped to establish the reaction pattern of the photoexcited ZnPc–C_{60}, namely, electron transfer from ZnPc to C_{60} through the optical signatures of the corresponding one-electron-oxidized radical cation and one-electron-reduced radical anion at 520, 840, and 1000 nm, respectively. Complementary density functional calculations confirm this assignment by virtue of the excitation spectra of ZnPc$^{\bullet+}$ and $C_{60}^{\bullet-}$, revealing strong excitation bands near 421 and 696 nm due to the ZnPc$^{\bullet+}$ moiety, and bands of somewhat lower intensity near 420, 546, 809, and 989 nm due to the $C_{60}^{\bullet-}$ fragment. Charge separation was found to be accelerated in the polar media, although the quantum yield of the charge separation is reduced in polar solvents (benzonitrile) relative to less-polar media (anisole). A similar trend was established for the charge-recombination process, which can be rationalized within the framework of the Marcus theory on electron transfer, that is, a decrease in rate constant as driving force increases.[27] In fact, Figure 13 corroborates this assumption providing values for the reorganization energy and electronic coupling of 0.61 eV and 5.9 cm^{-1}, respectively.

In the ZnPc–C_{60} conjugates, a competing intersystem crossing to the corresponding triplet manifold cannot be ruled out, albeit in very low quantum yields. This assessment
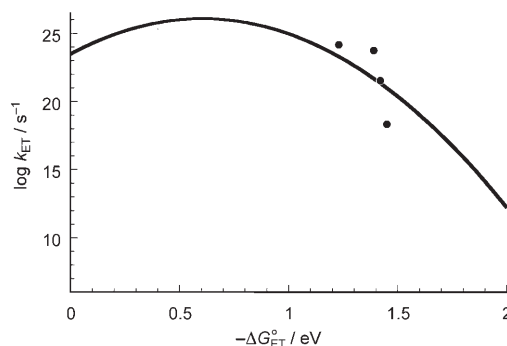

Figure 13. Driving-force ($-\Delta G^\circ_{ET}$) dependence of intramolecular electron transfer-rate constants in **2** (charge recombination: ●).

is based on 1) a kinetic comparison and 2) the fact that no clear evidence for triplet–triplet absorption was found, although the extinction coefficient for the ZnPc triplet excited state was reported between 18000 and 30000 M^{-1} cm^{-1}.[28] Although the impact of the linker (single, double, or triple bond) on the charge separation and charge-recombination features is rather marginal, the triple-bonded system (**1a**) is, nevertheless, showing the longest lifetime of the radical ion-pair state. Interestingly, the difference between the double-bonded (**1b**) and triple-bonded system (**1a**) resembles the trend seen in *p*-phenylenevinylene and *p*-phenyleneethyn-ylene.[29]

Experimental Section

General: UV/Vis spectra were recorded by using a Hewlett–Packard 8453 and Varian Cary 4E instruments. IR spectra were recorded by using a Bruker Vector 22 spectrophotometer. MALDI-TOF MS and HRMS spectra were recorded by using a Bruker Reflex III spectrometer. NMR spectra were acquired from Bruker AC-300 and AC-500 instruments. Column chromatographies were carried out on silica gel Merck-60 (230–400 mesh, 60 Å), and TLC on aluminum sheets precoated with silica gel 60 F_{254} (E. Merck). Chemicals were purchased from Aldrich Chemical Co. and were used as received without further purification. Iodo-substituted ZnPc **4** was prepared according to published procedures.[9] Photophysics: Steady-state fluorescence measurements were performed by using a Fluoromax 3 (Horiba Jobin Yvon). Transient absorption experiments, based on nanosecond laser photolysis, were performed with the output of the third harmonics (355 nm) coming from a Nd/YAG laser (Brilliant, Quantel). Moreover, pulse widths of <5 ns with an energy of 10 mJ were selected. The optical detection is based on a pulsed Xenon lamp (XBO 450, Osram), a monochromator (Spectra Pro 2300i, Acton Research), a R928 photomultiplier tube (Hamamatsu Photonics), or a fast InGaAs photodiode (Nano 5, Coherent) with 500-MHz amplification and a 1-GHz digital oscilloscope (WavePro7100, LeCroy). The laser power of every laser pulse was registered by using a bypath with a fast silicon photodiode. The solvents were always of spectroscopic grade. The ns-laser photolysis experiments were performed by using 1-cm quartz cells and the solutions were saturated with argon if no other gas saturation is indicated. The femtosecond transient absorption measurements were carried out with a CPA-2001 femtosecond laser (Clark MXR). The excitation wavelength was generated with an NOPA (Clark MXR); pulse widths <150 fs with an energy of 240 nJ were selected.

2,9,16-Tri-*tert*-butyl-23-(3-hydroxy-1-propynyl)phthalocyaninatozinc(II) (5): Tri-*tert*-butyliodophthalocyaninatozinc(II) (**4**) (100 mg, 0.11 mmol), [Pd(PPh₃)₂Cl₂] (8 mg, 0.011 mmol), and CuI (4 mg, 0.02 mmol) were dissolved in a mixture of freshly distilled Et₃N (0.5 mL) and dry THF (4 mL), under argon atmosphere. Propargyl alcohol (13 µL, 0.22 mmol) was added to this stirred solution, and the reaction was allowed to proceed at RT for 20 h. The solvent was removed under vacuum and the residual solid was dissolved in CHCl₃, washed with water and dried over Na₂SO₄. After filtration of the drying agent, the solvent was vacuum-evaporated and the crude product was subjected to column chromatography on silica gel using hexane/dioxane (3:1) as eluent to afford **5** as a blue solid, in the form of a mixture of regioisomers in 63% yield (55.4 mg). M.p. >250°C; ¹H NMR (300 MHz, [D₆]DMSO, 25°C, TMS): δ = 9.4–8.1 (m, 12H; arom. H), 4.6 (br, 2H; CH₂OH), 3.7–3.3 (br s, 1H; OH), 1.8 ppm (m, 27H; C(CH₃)₃); IR (KBr): $\tilde{v}$ = 2954, 2154, 1456, 1385, 1273, 1089, 1038, 919, 865, 829, 764, 746, 691, 670, 600 cm⁻¹; UV/Vis (CHCl₃): λ_{max} (log ε) = 684 (5.02), 614 (4.28), 352 nm (4.73); MALDI-TOF-MS (dithranol): m/z: 799.3 [M+H]⁺; HR-MALDI-TOF-MS (dithranol): m/z: calcd for C₄₇H₄₂N₈OZn: 798.2767 [M+H]⁺; found: 798.2788.

2,9,16-Tri-*tert*-butyl-23-(2-formylethynyl)phthalocyaninatozinc(II) (6): Phthalocyanine **5** (50 mg, 0.062 mmol) was dissolved in anhydrous CH₂Cl₂ (10 mL) and added in one portion to a suspension of PCC (40 mg, 0.102 mmol) in anhydrous CH₂Cl₂ (10 mL). The mixture was stirred for 24 at room temperature, and then filtered over Celite. After the solvents were evaporated under reduced pressure, the residual solid was extracted with CHCl₃, dried over Na₂SO₄ and purified by column chromatography on silica gel using hexane/dioxane (3:1) as eluent to afford phthalocyanine **6** as a green solid in the form of a mixture of regioisomers in 47% yield (23.3 mg). M.p. >250°C; ¹H NMR (300 MHz, [D₆]DMSO, 25°C, TMS): δ = 9.8 (s, 1H; CHO), 9.4–8.1 (br, 12H; arom. H), 1.9 ppm (m, 27H; C(CH₃)₃); IR (KBr): $\tilde{v}$ = 2955, 2861, 2181, 1658 (CO), 1611, 1486, 1386, 1364, 1330, 1280, 1256, 1148, 1086, 1046, 989, 920, 830, 747, 672 cm⁻¹; UV/Vis (CHCl₃): λ_{max} (log ε) = 700 (5.08), 672 (5.04), 641 (4.54), 612 (4.40), 354 nm (4.86); MALDI-TOF-MS (dithranol): m/z: 797.3 [M+H]⁺; HR-MALDI-TOF-MS (dithranol): m/z: calcd for C₄₇H₄₀N₈OZn: 796.26111 [M+H]⁺; found: 796.26135.

2,9,16-Tri-*tert*-butyl-23-(2-formylethenyl)phthalocyaninatozinc(II) (7): A solution of iodophthalocyanine **4** (40 mg, 0.046 mmol), acrolein (0.8 mL, 12 mmol), NaHCO₃ (16.8 mg, 0.2 mmol), tetra-*n*-butylammonium chloride (22 mg, 0.08 mmol), and [Pd(OAc)₂] (2 mg, 0.009 mmol) in anhydrous DMF (3 mL) was stirred at RT under argon atmosphere for 48 h. Water was added to the reaction mixture and the organic layer was extracted with ethyl acetate, dried over Na₂SO₄, filtered and evaporated. The crude was purified by column chromatography on silica gel using hexane/dioxane (3:1) as eluent. Compound **7** was obtained as a green solid in the form of a mixture of regioisomers in 91% yield (33.4 mg). M.p. >250°C; ¹H NMR (500 MHz, [D₆]DMSO, 25°C, TMS): δ = 10.1–9.9 (m, 1H; CHO), 9.4–8.1 (m, 12H; arom. H), 7.4–7.2 (br m, 2H; vinyl H), 1.8 ppm (m, 27H; C(CH₃)₃); IR (KBr): $\tilde{v}$ = 2954, 1677 (CO), 1607, 1458, 1385, 1330, 1280, 1256, 1122, 1087, 1046, 976, 920, 865, 761, 747, 672, 598 cm⁻¹; UV/Vis (CHCl₃): λ_{max} (log ε) = 702 (5.10), 675 (5.05), 642 (4.56), 353 nm (4.86); MALDI-TOF-MS (dithranol): m/z: 799.3 [M+H]⁺; HR-MALDI-TOF-MS (dithranol): m/z: calcd for C₄₇H₄₀N₈OZn: 798.2767 [M+H]⁺; found: 798.2768.

2,9,16-Tri-*tert*-butyl-23-(2-formylethyl)phthalocyaninatozinc(II) (8): A solution of iodophthalocyanine **4** (70 mg, 0.08 mmol), allylic alcohol (16 µL, 0.24 mmol), NaHCO₃ (16.8 mg, 0.2 mmol), tetra-*n*-butylammonium chloride (22 mg, 0.08 mmol), and [Pd(OAc)₂] (1.1 mg, 0.0045 mmol) in anhydrous DMF (2 mL) was stirred at RT under argon atmosphere for 48 h. Water was added to the reaction mixture and the organic layer was extracted with ethyl acetate, dried over Na₂SO₄, filtered and evaporated. The crude was purified by column chromatography on silica gel with hexane/dioxane (4:1) as eluent. Compound **8** was obtained as a blue solid in the form of a mixture of regioisomers in 76% yield (48.8 mg). M.p. >250°C; ¹H NMR (300 MHz, [D₆]acetone, 25°C, TMS): δ = 10.0 (s, 1H; CHO), 9.4–8.0 (m, 12H; arom. H), 3.5–3.3 (br m, 2H; CH₂CH₂CHO), 3.2–3.1 (br m, 2H; CH₂CH₂CHO), 1.7–1.5 ppm (m, 27H; C(CH₃)₃); IR (KBr): $\tilde{v}$ = 2954, 2865, 1720 (CO), 1677, 1612, 1487, 1392, 1363, 1331, 1280, 1256, 1147, 1088, 1047, 921, 829, 761, 746, 671 cm⁻¹; UV/Vis (CHCl₃): λ_{max} (log ε) = 678 (5.11), 612 (4.48), 350 nm (4.81); MALDI-TOF-MS (dithranol): m/z: 800.3 [M]⁺; HR-MALDI-TOF (dithranol): m/z: calcd for C₄₇H₄₄N₈OZn: 800.2924 [M]⁺; found: 800.2907.

General procedure for the preparation of conjugates 1a–c: A dry toluene solution (50 mL) of C₆₀ fullerene (94 mg, 0.131 mmol), *N*-methylglycine (19.6 mg, 0.22 mmol), and the corresponding formylphthalocyanine **6–8** [**6** (for **1a**), **7** (for **1b**), and **8** (for **1c**)] (0.044 mmol) was heated to reflux under argon atmosphere for 20 h. The solution was then cooled to RT and concentrated under vacuum to a volume of approximately 10 mL. The resulting mixture was poured onto a silica-gel column and eluted with toluene/ethyl acetate 95:5, passing to toluene/ethyl acetate 8:1, in order to separate the monoaddition products from the bisadducts and unreacted fullerene. Further purification of the monoadducts was achieved by washing the solid products with acetone, methanol, and hexane.

ZnPc–C₆₀ conjugate 1a: Intense-green solid; 13.6 mg (20%); m.p. >250°C; ¹H NMR (300 MHz, [D₈]THF, 25°C, TMS): δ = 9.6–8.2 (m, 12H; arom. H), 5.6, 5.1, and 4.5 (br, 3H; pyrrolidine H), 3.0 (s, 3H; N-CH3), 1.9 ppm (m, 27H; C(CH₃)₃); IR (KBr): $\tilde{v}$ = 2957, 1613, 1455, 1384, 1261, 1088, 1039, 921, 865, 802, 748, 670, 600, 527 cm⁻¹; UV/Vis (CHCl₃): λ_{max} (log ε) = 689 (5.14), 678 (5.12), 615 (4.51), 351 (4.96), 255 nm (5.11);

MALDI-TOF MS (dithranol): m/z: 1545.4 $[M]^+$, 823.5 $[M-C_{60}]^+$; HR-MALDI-TOF-MS (dithranol): m/z: calcd for $C_{109}H_{45}N_9Zn$: 1543.3084 $[M]^+$; found: 1543.3025.

ZnPc–C$_{60}$ conjugate 1b: Intense-green solid; 15.7 mg (23%); m.p. >250°C; ^{1}H NMR (300 MHz, $[D_8]$THF, 25°C, TMS): $\delta = 9.7$–8.4 (m, 12H; arom. H), 7.2–7.0 (br, 2H; vinyl H), 5.1, 4.8, and 4.3 (br, 3H; pyrrolidine H), 3.1 (s, 3H; N-CH$_3$), 1.9 ppm (m, 27H; C(CH$_3$)$_3$); IR (KBr): $\tilde{\nu} =$ 2957, 2776, 1613, 1455, 1261, 1088, 1039, 921, 865, 801, 748, 670, 600, 526 cm^{-1}; UV/Vis (CHCl$_3$): λ_{max} (log ε) = 686 (5.17), 617 (4.51), 350 (4.94), 257 nm (5.12); MALDI-TOF MS (dithranol): m/z: 1548.1 $[M+H]^+$, 825.3 $[M-C_{60}]^+$; HR-MALDI-TOF-MS (dithranol): m/z: calcd for $C_{109}H_{47}N_9Zn$: 1545.3240 $[M+H]^+$; found: 1545.3204.

ZnPc–C$_{60}$ conjugate 1c: Intense-green solid; 14.3 mg (21%); m.p. >250°C; ^{1}H NMR (500 MHz, $[D_8]$THF, 25°C, TMS): $\delta = 9.6$–8.2 (m, 12H; arom. H), 5.0, 4.4, and 3.9 (m, 3H; pyrrolidine H), 3.2 (s, N-CH$_3$), 2.6–2.4 (m, 2H; CH$_2$CH$_2$), 1.9–1.6 ppm (2×m, 29H; CH$_2$CH$_2$ and C-(CH$_3$)$_3$); IR (KBr): $\tilde{\nu} =$ 2956, 1613, 1385, 1272, 1089, 1039, 921, 865, 800, 748, 670, 601, 527 cm^{-1}; UV/Vis (CHCl$_3$): λ_{max} (log ε) = 679 (5.22), 613 (4.45), 346 (4.91), 256 nm (5.10); MALDI-TOF MS (dithranol): m/z: 1549.5 $[M]^+$, 827.5 $[M-C_{60}]^+$; HR-MALDI-TOF-MS (dithranol): m/z: calcd for $C_{109}H_{49}N_9Zn$: 1547.3397 $[M]^+$; found: 1547.3418.

Acknowledgements

[1] a) *The Photosynthetic Reaction Center* (Eds.: J. Deisenhofer, J. R. Norris), Academic Press, New York, **1993**; b) *Electron Transfer in Chemistry, Vol. I–V* (Ed.: V. Balzani), Wiley-VCH, Weinheim, **2001**; c) N. Sutin, *Acc. Chem. Res.* **1982**, *15*, 275; d) *Photoinduced Electron Transfer* (Eds.: M. A. Fox, M. Chanon), Elsevier, Amsterdam, **1988**; e) T. J. Meyer, *Acc. Chem. Res.* **1989**, *22*, 163; f) V. Balzani, F. Scandola in *Supramolecular Photochemistry*, Ellis Horwood, Chichester, **1991**, pp. 161–196, 355–394; g) M. R. Wasielewski, *Chem. Rev.* **1992**, *92*, 435; h) M. N. Paddon-Row, *Acc. Chem. Res.* **1994**, *27*, 18; i) A. J. Bard, M. A. Fox, *Acc. Chem. Res.* **1995**, *28*, 141; j) S. Speiser, *Chem. Rev.* **1996**, *96*, 1953; k) J. G. Calbert in *Photochemistry*, Wiley, **1996**; l) D. Gust, *Nature* **1997**, *386*, 21.

[2] Recent reviews: a) D. M. Guldi, M. Prato, *Acc. Chem. Res.* **2000**, *33*, 695; b) D. M. Guldi, *Chem. Commun.* **2000**, 321; c) D. Gust, T. A. Moore, A. L. Moore, *Acc. Chem. Res.* **2001**, *34*, 40; d) D. M. Guldi, *Chem. Soc. Rev.* **2002**, *31*, 22; e) N. Armaroli, *Photochem. Photobiol. Sci.* **2003**, *2*, 73; f) H. Imahori, Y. Mori, Y. Matano, *J. Photochem. Photobiol. C* **2003**, *4*, 51; g) S. Chakraborty, T. J. Wadas, H. Hester, R. Schmehl, R. Eisenberg, *Inorg. Chem.* **2005**, *44*, 6865; h) M. Grätzel, *Inorg. Chem.* **2005**, *44*, 6841; i) D. M. Guldi, G. M. A. Rahman, C. Ehli, V. Sgobba, *Chem. Soc. Rev.* **2006**, *35*, 471; j) D. I. Schuster, K. Li, D. M. Guldi, *Comptes Rendus Chim.* **2006**, *9*, 892.

[3] a) *Fullerenes: Principles and Applications* (Eds.: F. Langa, J.-F. Nierengarten), Royal Society of Chemistry, Oxford, **2007**; b) A. Hirsch, M. Brettreich in *Fullerenes: Chemistry and Reactions*, Wiley-VCH, Weinheim, **2004**; c) D. M. Guldi, N. Martín in *Fullerenes: From Synthesis to Optoelectronic Properties; Series: Developments in Fullerene Science*, Kluwer Academic, Dordrecht, **2002**.

[4] a) S. Fukuzumi, K. Ohkubo, O. Wenbo, Z. Ou, J. Shao, K. M. Kadish, J. A. Jutchison, K. P. Ghiggino, P. J. Sintic, M. J. Crossley, *J. Am. Chem. Soc.* **2003**, *125*, 14984; b) L. R. Sutton, M. Scheloske, K. S Pirner, A. Hirsch, D. M. Guldi, J. P. Gisselbrecht, *J. Am. Chem. Soc.* **2004**, *126*, 10370; c) M.-S. Choi, T. Yamazaki, I. Yamazaki, T.

Aida, *Angew. Chem.* **2004**, *116*, 152; *Angew. Chem. Int. Ed.* **2004**, *43*, 150; d) M. E. El-Khouly, O. Ito, P. M. Smith, F. D'Souza, *J. Photochem. Photobiol. C* **2004**, *5*, 79; e) F. D'Souza, O. Ito, *Coord. Chem. Rev.* **2005**, *249*, 1410.

[5] a) G. de la Torre, C. G. Claessens, T. Torres, *Chem. Commun.* **2007**, 2000; b) *Phthalocyanines: Properties and Applications, Vol. 1–4* (Eds.: C. C. Leznoff, A. B. P. Lever), VCH, Weinheim, **1989**, **1993**, **1996**; c) *The Porphyrin Handbook, Vol. 15–20* (Eds.: K. M. Kadish, K. M. Smith, R. Guilard), Academic Press, San Diego, **2003**; d) G. de la Torre, P. Vázquez, F. Agulló-López, T. Torres, *Chem. Rev.* **2004**, *104*, 3723.

[6] a) J. A. Duro, T. Torres, *Chem. Ber.* **1993**, *126*, 269; b) G. de la Torre, C. G. Claessens, T. Torres, *Eur. J. Org. Chem.* **2000**, 2821; c) A. de la Escosura, M. V. Martínez-Díaz, P. Thordarson, A. E. Rowan, R. J. M. Nolte, T. Torres, *J. Am. Chem. Soc.* **2003**, *125*, 12300; d) D. González-Rodríguez, T. Torres, D. M. Guldi, J. Rivera, M. A. Herranz, L. Echegoyen, *J. Am. Chem. Soc.* **2004**, *126*, 6301; e) M. Quintiliani, E. M. Garcia-Frutos, A. Gouloumis, P. Vázquez, I. Ledoux-Rak, J. Zyss, C. G. Claessens, T. Torres, *Eur. J. Org. Chem.* **2005**, 3911; f) A. Gouloumis, D. González-Rodríguez, P. Vázquez, T. Torres, S. Liu, L. Echegoyen, J. Ramey, G. L. Hug, D. M. Guldi, *J. Am. Chem. Soc.* **2006**, *128*, 12684; g) M. S. Rodríguez-Morgade, T. Torres, C. Atienza-Castellanos, D. M. Guldi, *J. Am. Chem. Soc.* **2006**, *128*, 15145; h) D. González-Rodríguez, T. Torres, M. M. Olmstead, J. Rivera, M. A. Herranz, L. Echegoyen, C. Atienza-Castellanos, D. M. Guldi, *J. Am. Chem. Soc.* **2006**, *128*, 10680; i) B. Ballesteros, G. de la Torre, C. Ehli, G. M. A. Rahman, F. Agulló-Rueda, D. M. Guldi, T. Torres, *J. Am. Chem. Soc.* **2007**, *129*, 5061.

[7] a) A. Sastre, A. Gouloumis, P. Vázquez, T. Torres, V. Doan, B. J. Schwartz, F. Wudl, L. Echegoyen, J. Rivera, *Org. Lett.* **1999**, *1*, 1807; b) A. Gouloumis, S.-G. Liu, A. Sastre P. Vázquez, L. Echegoyen, T. Torres, *Chem. Eur. J.* **2000**, *6*, 3600; c) D. M. Guldi, A. Gouloumis, P. Vázquez, T. Torres, *Chem. Commun.* **2002**, 2056; d) M. A. Loi, H. Neugebauer, P. Denk, C. J. Brabec, N. S. Sariciftci, A. Gouloumis, P. Vázquez, T. Torres, *J. Mater. Chem.* **2003**, *13*, 700; e) D. M. Guldi, I. Zilberman, A. Gouloumis, P. Vázquez, T. Torres, *J. Phys. Chem. B* **2004**, *108*, 18485; f) A. Gouloumis, A. de la Escosura, P. Vázquez, T. Torres, A. Kahnt, D. M. Guldi, H. Neugebauer, C. Winder, M. Drees, N. S. Sariciftci, *Org. Lett.* **2006**, *8*, 5187.

[8] a) D. M. Guldi, J. Ramey, M. V. Martínez-Díaz, A. de la Escosura, T. Torres, T. Da Ros, M. Prato, *Chem. Commun.* **2002**, 2774; b) D. M. Guldi, A. Gouloumis, P. Vázquez, T. Torres, V. Georgakilas, M. Prato, *J. Am. Chem. Soc.* **2005**, *127*, 5811; c) J. L. Sessler, J. Jayawickramarajah, A. Gouloumis, T. Torres, D. M. Guldi, S. Maldonado, K. J. Stevenson, *Chem. Commun.* **2005**, 1892; d) A. de la Escosura, M. V. Martínez-Díaz, D. M. Guldi, T. Torres, *J. Am. Chem. Soc.* **2006**, *128*, 4112; e) B. Ballesteros, G. de la Torre, T. Torres, G. L. Hug, G. M. A. Rahman, D. M. Guldi, *Tetrahedron* **2006**, *62*, 2097; f) T. Torres, A. Gouloumis, D. Sánchez-García, J. Jayawickramarajah, W. Seitz, D. M. Guldi, J. L. Sessler, *Chem. Commun.* **2007**, 292.

[9] E. M. Maya, P. Vázquez, T. Torres, *Chem. Eur. J.* **1999**, *5*, 2004.

[10] a) T. C. Zebovitz, R. F. Heck, *J. Org. Chem.* **1977**, *42*, 3907; b) P. Y Johnson, . J. Q. Wen, *J. Org. Chem.* **1981**, *46*, 2767; c) G. Battistuzzi, S. Cacchi, G. Fabrizi, *Org. Lett.* **2003**, *5*, 777.

[11] T. Jeffery, *J. Chem. Soc. Chem. Commun.* **1984**, 1287.

[12] a) T. Jeffery, *Tetrahedron Lett.* **1991**, *32*, 2121; b) T. Jeffery, *J. Chem. Soc. Chem. Commun.* **1991**, 324; c) T. Jeffery, *Tetrahedron Lett.* **1993**, *34*, 1133; d) T. Jeffery, *Tetrahedron Lett.* **1990**, *31*, 6641.

[13] G. Ricciardi, A. Rosa, E. J. Baerends, *J. Phys. Chem. A* **2001**, *105*, 5242.

[14] P. S. Vincett, E. M. Voigt, K. E. Rieckhoff, *J. Chem. Phys.* **1971**, *55*, 4131.

[15] a) S. FitzGerald, C. Farren, C. F. Stanley, A. Beeby, M. R. Bryce, *Photochem. Photobiol. Sci.* **2002**, *1*, 581; b) C. Farren, S. FitzGerald, A. Beeby, M. R. Bryce, *Chem. Commun.* **2002**, 572.

[16] S. H. Gallagher, R. S. Armstrong, P. A. Lay, C. A. Reed, *J. Phys. Chem.* **1995**, *99*, 5817.

[17] a) M.-S. Liao, S. Scheiner, *J. Chem. Phys.* **2001**, *114*, 9780; b) K. A. Nguyen, R. Pachter, *J. Chem. Phys.* **2001**, *114*, 10757; c) A. Rosa, G. Ricciardi, O. Gritsenko, E. Baerends, *Structure and Bonding* **2004**, *112*, 49.

[18] The five most intense excitations are centered around an excitation wavelength of 270 nm, which is outside the experimental range of detection, and hence their discussion is omitted here (for details, see Table S2).

[19] All of these excitations show considerable configuration mixing.

[20] a) M. E. El-Khouly, O. Ito, P. M. Smith, F. D'Souza, *J. Photochem. Photobiol. C* **2004**, *5*, 79; b) T. Nyokong, Z. Gasyna, M. Stillman, *Inorg. Chem.* **1987**, *26*, 548.

[21] Z. Gasyna, L. Andrews, P. N. Schatz, *J. Phys. Chem.* **1992**, *96*, 1525.

[22] I. Carmichael, W. P. Helman, G. L. Hug, *J. Phys. Chem. Ref. Data* **1987**, *16*, 239.

[23] C. Tanielian, C. Wolff, *J. Phys. Chem.* **1995**, *99*, 9831.

[24] T. Ohno, S. Kato, N. N. Lichtin, *Bull. Chem. Soc. Jpn.* **1982**, *55*, 2753.

[25] a) R. A. Marcus, *J. Chem. Phys.* **1956**, *24*, 966; b) R. A. Marcus, *J. Chem. Phys.* **1957**, *26*, 867; c) E. Akesson, G. C. Walker, P. F. Bar-

bara, *J. Chem. Phys.* **1991**, *95*, 4188; d) T. Ichiye, *J. Chem. Phys.* **1996**, *104*, 7561.

[26] For consistency, the companion excitations to 54A and 55A within the majority spin channel (α, labeled 39A and 40A), which are of considerably lower intensity, have also been included in Table S5.

[27] a) R. A. Marcus, *J. Chem. Phys* **1956**, *24*, 966; b) R. Marcus, N. Sutin, *Biochim. Biophys. Acta* **1985**, *811*, 265.

[28] a) S. M. Bishop, A. Beeby, H. Meunier, A. W. Parker, M. S. C. Foley, D. Philips, *J. Chem. Soc. Faraday Trans.* **1996**, *92*, 2689; b) M. Aoudia, G. Cheng, V. O. Kennedy, M. E. Kenney, J. M. A. Rodgers, *J. Am. Chem. Soc.* **1997**, *119*, 6029.

[29] a) F. Giacalone, J. L. Segura, N. Martín, D. M. Guldi, *J. Am. Chem. Soc.* **2004**, *126*, 5340; b) C. Atienza-Castellanos, N. Martín, M. Wielopolski, N. Haworth, T. Clark, D. M. Guldi, *Chem. Commun.* **2006**, 3202.